Received: 3 October 2019 | Revised: 5 June 2020 | Accepted: 8 June 2020

DOI: 10.1002/sia.6854

ECASIA SPECIAL ISSUE PAPER

SURFACE and INTERFACE ANALYSIS WILEY

Surface analysis of bacterial systems using cryo-X-ray photoelectron spectroscopy

Aleksandra Hagberg[1] | Olena Rzhepishevska[1] | Anastasiia Semenets[1,2] | David A. Cisneros[3] | Madeleine Ramstedt[1]

[1]Department of Chemistry, UCMR, Umeå University, Umeå, Sweden

[2]Department of Microbiology, Virology and Biotechnology, Odessa National I.I.Mechnikov University, Odessa, Ukraine

[3]Department of Molecular Biology, UCMR, Umeå University, Umeå, Sweden

Correspondence
Madeleine Ramstedt, Department of Chemistry, UCMR, Umeå University, 901 87. Umeå, Sweden.
Email: madeleine.ramstedt@umu.se

Funding information
Formas, Grant/Award Number: 2017-00403; Kempe Foundation, Grant/Award Number: JCK-1720

Surface analysis of biological systems using XPS often requires dehydration of the sample for it to be compatible with the ultrahigh vacuum of the spectrometer. However, if samples are frozen to liquid-nitrogen temperature prior to and during analysis, water can be retained in the sample and the organization of the sample surface should be preserved to a higher degree than in desiccated samples. This article presents recent developments of cryo-X-ray photoelectron spectroscopy (cryo-XPS) for analyses of hydrated biological samples at liquid nitrogen temperature. We describe experiments on bacterial cells, bacterial biofilms, and bacterial outer membrane vesicles using a variety of bacterial species. Differences and similarities in surface chemistry are monitored depending on growth in liquid culture, on culture plates, as well as in biofilms, and are discussed. Two data treatment methods providing decomposition of the C 1s spectra into lipid, polysaccharide, and peptide/peptidoglycan content are used and compared.

1 | INTRODUCTION

Bacterial interactions with their surrounding environment are mediated through their cell envelope, as well as other bacterial surface structures such as flagella and fimbriae.[1] These interactions are complex and rely on several factors including physicochemical interactions and specific molecular recognition mechanisms mediated through receptors.[2–4] To investigate these complex systems, analyses of the surface chemistry can be a useful tool in order to better understand and interpret processes involving the cell surface. For example, an increase in protein concentration at the surface of some bacteria, may indicate spore formation,[5] increased amounts of membrane proteins, or other types of adaptations. Differences in polysaccharide content may indicate changes in the lipopolysaccharide composition of the outer membrane in Gram-negative bacteria,[6] or be a result of altered expression of capsules or surface-bound extracellular substances. In this context, X-ray photoelectron spectroscopy (XPS) is an attractive analysis technique, as its surface sensitivity enables analyses of only the outermost part of the cell envelope of bacteria and/or surface appendages and coatings,[6] thereby enabling characterization of the cell envelope without influence from the cytoplasmic content of the bacterial cell. However, this is only valid if sample pretreatment methods keep the cells intact (i.e., does not rupture or beak them exposing their interior or causing building blocks to migrate in the cell-envelope structure).

Bacteria have several "lifestyles" (free-swimming planktonic cells, sessile cells, etc.) depending on factors such as stress levels, nutrient supply, and interactions with other (micro) organisms. Often these lifestyles can be correlated to metabolic differences.[7,8] Thus, planktonic cells cultivated in liquid broth may differ in surface composition compared with cells growing on a solid nutrient medium such as an nutrient agar plate or cells growing inside a biofilm.[9] Biofilms are coatings formed by bacterial cells embedded in a matrix of substances that they have secreted, so-called extracellular polymeric substances (EPS).[7] Bacteria inside biofilms display lower susceptibility to antibiotics and biocides as a result of several factors including changes in

metabolic activity and that they are shielded from the environment by the EPS.[7,8] Bacterial cells, both in planktonic form and in biofilms, can release small parts of their cell membranes forming membrane vesicles (that also can be analyzed using XPS). These have been suggested to play a range of roles including cell-cell communication, nutrient uptake, scavenging of toxins, and as toxin-delivery vehicles.[10] In Gram-negative bacteria, these vesicles are called outer-membrane vesicles (OMVs) as they mainly originate from the outer membrane that buds and forms vesicles.[10,11] Also, Gram-positive bacteria form membrane vesicles, but the mechanism behind that process is less understood, although well documented.[11,12]

1.1 | Short historic perspective on data treatment

Bacterial cells have been analyzed using XPS for several decades using freeze-dried or dehydrated samples to enable compatibility with high-vacuum XPS systems.[13,14] These analyses have provided useful biochemical characterization of the cell envelope. The building blocks of the bacterial cell envelope mainly consist of different types of carbon-based substances, such as lipids, polysaccharides, proteins, and peptidoglycans, which are all contributing to the C 1s spectrum of a bacterial sample. In order to estimate the surface composition based on these substance groups, Rouxhet and Genet[15] developed two equation systems based on (1) the elemental ratio of C, N, and O (Equations 1a-1c) and (2) ratios between different components within the C 1s spectrum (Equations 2a-2c).

Equations 1:

$$[N/C]_{obs} = 0.279(C_{Pr}/C) \quad (1a)$$

$$[O/C]_{obs} = 0.325\,(C_{Pr}/C) + 0.833\,(C_{PS}/C) \quad (1b)$$

$$[C/C]_{obs} = 1 = (C_{Pr}/C) + (C_{PS}/C) + (C_{HC}/C) \quad (1c)$$

Equations 2:

$$[C_{288.2}/C]_{obs} = 0.279(C_{Pr}/C) + 0.167(C_{PS}/C) \quad (2a)$$

$$[C_{286.4}/C]_{obs} = 0.293(C_{Pr}/C) + 0.833(C_{PS}/C) \quad (2b)$$

$$[C_{285.0}/C]_{obs} = 0.428(C_{Pr}/C) + 1(C_{HC}/C) \quad (2c)$$

where obs is observed, C_{PS} is polysaccharide, C_{Pr} is protein/peptidoglycan, and C_{HC} is hydrocarbon.

The first equation system (Equations 1a-1c) is not applicable for biological cryo-XPS data, as O 1s spectra of frozen hydrated cells will contain large amounts of water that is not well correlated to the substance composition of the bacterial cell. Therefore, in 2011, we developed a method using three mathematically derived components to fit the C 1s spectra of bacteria in order to predict the amounts of lipid, polysaccharide, and peptide (protein + peptidoglycan).[6] These components were constructed through the use of multivariate curve resolution of 42 samples (35 Gram-negative *Escherichia coli* bacterial samples with differences in cell envelope composition as well as seven standards) where we found that three components could reproduce 99.7% of the variance observed in the dataset.[6] These mathematical components (here called spectral components) were later used to predict the surface composition of a set of Gram-positive bacterial samples, showing that cryo-XPS could be used to monitor changes in the cell wall of *Bacillus subtilis* bacteria exposed to different growth environments (changes in solution pH and metal content). The substance composition obtained using this new method was, furthermore, compared with the two equation systems showing that the two different data treatment methods give similar albeit not identical results.[5,16] However, for hydrated fast-frozen samples, only Equations 2a to 2c and the model with spectral components are applicable.

For analysis of bacterial samples, cryo-XPS analyses are here suggested as preferable to analysis of dried specimens as the fast-frozen sample surface should maintain a structural arrangement more similar to what would be encountered in a hydrated situation.[5,17] The removal of water during dehydration of bacterial samples may induce cell rupture and/or reorganization of cell envelope constituents. This hypothesis was previously supported by analyses performed on bacterial samples that were first analyzed frozen and thereafter left to slowly dehydrate in vacuum before a second analysis of the dehydrated cell. In some samples (but not all) very large changes could be observed in the carbon composition, suggesting increased amount of lipid-like substances after dehydration.[5]

In this paper, we describe how we have applied the method of cryo-XPS to different types of (hydrated and frozen) bacterial systems and discuss sample preparation and data treatment.

2 | MATERIALS AND METHODS

Bacterial strains from the species *Rahnella aquatilis*, *Pseudomonas fluorescens*, *Pseudomonas aeruginosa*, and *E. coli* (Table 1) were individually defrosted from −80°C glycerol stocks and cultivated separately on agar plates. All bacteria were cultivated on Luria-broth (LB) medium except the river isolate *R. aquatilis* that was cultivated on R2A medium, ie, a medium for microorganisms emulating nutrient-poor fresh water.[22] This strain was isolated from immersed plant material in the Knivstån, Sweden (coordinates from Google: lat 59.72; long 17.79) in June 2018 downstream from the outlet of a sewage treatment plant (the strain was included here for its visibly large EPS production).

For analyses of morphology by regular SEM, *R. aquatilis* colonies grown on R2A agar plates were cut into small pieces and fixed with 2.5% glutaraldehyde in sodium cacodylate buffer and left overnight at 4°C. The samples were dehydrated in a series of graded ethanol (70%, 80%, 90%, 95%, and 100%) 10 minutes in each bath. Thereafter, the samples were critical-point dried and coated with 5 nm iridium. Morphology was analyzed by field-emission scanning electron microscopy (SEM; Carl Zeiss Merlin) using secondary electron detector at accelerating voltage of 5 kV and probe current of 120 pA. For cryo-SEM

TABLE 1 Bacterial strains used for studies of planktonic cells, biofilms, and OMVs

Species	Strain	Ref Number	Characteristic	Reference
Study of Planktonic Cells From Different Cultivation Modes				
R. aquatilis	River isolate	AH0123	EPS producer	This study
P. fluorescens		DSM50090	Reference strain	
P. fluorescens		CIP69.13	Reference strain	
Study of Biofilms vs Planktonic Cells				
P. aeruginosa	PAO1		Reference strain	[18]
P. aeruginosa	PAO1 *ΔpelA*		Polysaccharide (pel A) mutant	[19]
P. aeruginosa	PAO1 *ΔpJN2133*		Low c-di-GMP	[20]
P. aeruginosa	PAO1 *ΔwspF1*		High c-di-GMP	[20]
Study of OMVs vs Planktonic Cells				
E. coli	BW25113 *ΔflhD*	RN110	Flagella mutant	[21]
E. coli	BW25113 *ΔwaaL ΔflhD*	RN115	Double mutant in LPS and of flagella	[6]

analysis, colonies were deposited onto carbon adhesive tape mounted on a copper holder. Samples were subsequently vitrified in liquid nitrogen slush. Prior to imaging, the frozen sample was sublimated in vacuum for up to 30 minutes at −90°C. Imaging was performed on a Carl Zeiss Merlin field-emission cryogenic scanning electron microscope (cryo-FESEM), fitted with a Quorum Technologies PP3000T cryo preparation system. Images were collected at temperatures below 193 K using secondary electron detector (ETD) at an accelerating voltage of 2 kV and probe current of 50 pA. For AFM imaging, a bacterial colony from an agar plate was suspended in 100 μL miliQ water. A volume of 10 μL of the suspension was immobilized on freshly cleaved mica while gently drying in air. In a measurement where EPS was removed, a colony from an agar plate was washed twice in 1 mL miliQ water and centrifuged at 4000 RPM for 5 minutes and the supernatant discarded. Thereafter, the bacterial pellet was resuspended in 100 μL miliQ water and the bacteria were immobilized on freshly cleaved mica as described above. AFM analysis was done in a multimode 8 using with ScanAsyst (Bruker) in peak force tapping mode in air.

Cryo-XPS analyses, data treatment, and sample pretreatment were done according to previously published procedures.[5,6,23] Analyses were performed on a Kratos Axis Ultra DLD electron spectrometer using a monochromatic Al Kα source operated at 150 W. Spectra were analyzed using a hybrid lens system with a magnetic lens. Angle between the incident X-ray photon beam and analyzer was 57.4°, photoelectron takeoff angle 90°, and collection angle of the analyzer ±15°. Maximum photoemission from sample was at 90°. The analysis area was 0.3 × 0.7 mm (slot). An analyzer pass energy of 160 and 20 eV was used for survey spectra and high-resolution spectra, respectively. The sample introduction chamber and analysis chamber were both pre-cooled to liquid nitrogen temperature before sample introduction and analysis, and were kept cold throughout the measurement. Sample charging during measurements was compensated using the built-in spectrometer charge-neutralizing system. The C 1s hydrocarbon peak at 285.0 eV was thereafter used for calibration of the binding energy scale. Chemical constituents giving rise to intensity in the C 1s peak were predicted using three mathematical components describing lipids, polysaccharides, and peptide (protein + peptidoglycan), here called spectral components, ie, independently from classical curve fitting of C 1s spectra using Gaussian–Lorentzian peak shapes.[6] For comparison, substance compositions were also calculated using Equations 2a to 2c after peak fitting using CasaXPS. Statistics were calculated using the Student's *T* test in Excel.

Adaptations in sample treatment for cryo-XPS measurements were made for each of the five sample groups: bacterial cells from liquid culture (1), culture plates (2 and 3), OMVs (4), and biofilms (5) as described below. All samples were measured at least as two biological replicates and all, except biofilms, were measured "fast-frozen", ie, were applied onto a sample holder at room temperature, frozen instantaneously on the sample stage in the sample introduction chamber of the spectrometer, and analyzed in hydrated frozen form, as previously described.[17,23] The sample was maintained at liquid nitrogen temperature throughout the analysis time, and the vacuum in the analysis chamber carefully was monitored (generally 3–5 × 10^{-7} Pa). Bacterial cells were analyzed both from liquid culture (1) and from culture plates (2 and 3). Culture plates were freshly streaked with bacteria and incubated overnight at 37°C for *E. coli* or *P. aeruginosa* and for 2 days at room temperature (21°C) for *R. aquatilis* and *P. fluorescens*. (1) For liquid cultures, one or a few colonies were taken from a culture plate and inoculated into appropriate liquid medium. The culture was grown overnight under shaking (for slowly growing *R. aquatilis* and *P. fluorescens* 24 h). Thereafter, the suspension was centrifuged; the pellet was washed using phosphate-buffered saline (PBS) and once more centrifuged. A volume of ∼20 μL of the resulting pellet was used for XPS analyses. For XPS analysis of bacterial cells grown in liquid medium, this washing step is important so that C-containing substances from the growth medium are removed that else would end up in XPS spectra. The washing was performed using a buffer in order to maintain the same pH between all samples, as it has been shown that the bacterial surface composition may be altered depending on pH.[5]

PBS was chosen to avoid introducing any C-containing substance that would "contaminate" the C 1s spectrum. (2) Bacteria analyzed directly from plates were collected from freshly cultivated plates using a loop and the collected biomass was directly applied onto the sample holder or (3) suspended in 2 mL PBS, vortexed, centrifuged, and the washed pellet used for XPS analyses. OMVs (4) were isolated from bacterial cultures using previously described methods.[21,24] Bacterial strains without flagella were chosen to avoid having parts of broken flagella in the OMV preparation. The OMVs were suspended into PBS. Before analysis, this suspension was centrifuged and 20 μL of the pellet was transferred to the sample holder for XPS analysis. For samples where the vesicle pellet was too small to transfer from the test tube to the sample holder, the pellet was resuspended in a small volume of PBS, and a 20 μL drop of this vesicle-containing PBS solution was instead placed on a precooled sample holder inside the sample introduction chamber where it immediately froze (this latter procedure was used for the OMVs from *ΔflhD*). Biofilms (5) were cultivated on small glass cover slides by immersing glass slides sterilized for 30 minutes in 70% ethanol into LB culture medium and adding an aliquot of bacteria (0.5×10^6 cells/mL), thereafter incubating (static) for 12 or 15 hours at 37°C in 24-well plates (with cavities of appropriate size to contain the glass slides). The following day, the slides covered with biofilm were very gently rinsed in 0.9% NaCl and thereafter frozen and stored at −80°C. Freezing samples to −80°C directly after preparation enabled several samples to be prepared in parallel using identical conditions and thereafter conserved, for subsequent cryo-XPS analyses. On the day of analysis, the frozen sample was brought to the XPS in a sterile Petri dish on dry ice. A piece of the biofilm-covered glass was placed, still frozen, onto a sample holder precooled with liquid nitrogen. Thereafter, the sample holder was inserted into the analysis chamber as soon as possible (to limit water condensation on the cold metal). To take into account any spatial heterogeneities, three points were analyzed on each biofilm sample. After each analysis, sample and sample holder were sonicated in ethanol twice to clean, sterilize, and avoid sample contamination or carry-over.

3 | RESULTS AND DISCUSSION

3.1 | Planktonic cells

Bacterial cells grown in liquid culture or on a solid nutrient agar are sometimes both considered as planktonic cells, and may therefore display similar surface composition.[25] Consequently, XPS spectra of these two growth-forms may be similar, unless secretion of extracellular substances have taken place. To investigate this, we analyzed bacteria grown on culture plates and in liquid culture. We analyzed two different bacterial species: *P. fluorescens* (two reference strains DSM50090 and CIP69.13) and a Swedish river isolate (AH0123) of the species *R. aquatilis*. This river isolate was included as we observed that it produced very large quantities of EPS that was clearly visible by eye on culture plates as well as in liquid culture. This species is also known to have production of organic acids as well as extracellular polysaccharides of interest to industrial applications.[26–28] In cryo-SEM images, the secreted EPS is clearly observed as a layer in which the cells are dispersed (Figure 1A,B). Using regular SEM, the EPS layer dehydrates, collapses, and forms peculiar features (Figure 1C,D). AFM analyses showed that the EPS observed to cover the cells in the SEM analyses was removed to a large extent by washing, uncovering smooth rod-shaped bacteria with flagella (Figure 1E,F).

Cryo-XPS analyses of planktonic cells of *R. aquatilis* showed differences in C 1s spectra between replicates of nonwashed bacteria, giving rise to large error bars in Figure 2. We hypothesize that these differences result from sample variations in the ratio of EPS to bacteria, which is very difficult to control during sample transfer from the culture plate. Visual inspection of the culture plates showed individual colonies surrounded by large amounts of highly hydrated EPS. Bacteria grown in liquid culture (always washed) and the bacteria cultivated on plates and thereafter washed had similar surface compositions (Figure 2). AFM imaging of cells before and after wash (Figure 1E,F) indicates at least partial removal of EPS during washing. The differences observed between nonwashed and washed cells seemed to mainly involve the peptide and lipid components suggesting that the contents of these substances differ between cells and EPS. The washed cells appeared to display larger percentages of peptide, which may indicate an EPS with relatively high percentage of polysaccharide and lipid-like substances compared with the bacterial cell, in line with previous reports.[26]

The two strains of *P. fluorescens* (DSM50090 and CIP69.13) were significantly different in surface composition from each other ($p < 0.01$). Neither of them appeared to form large quantities of EPS by visual inspection of culture plates. Thus, the same chemical surface composition was obtained between bacteria grown in liquid culture and on culture plate or between washed and not washed cells (Figure 2 and Table 2). As an example, the DSM50090 strain analyzed directly from plate gave a composition of 67 ± 3% peptide, 7 ± 2% lipid, and 26 ± 2% polysaccharide, whereas the rinsed showed 65 ± 4% peptide, 9 ± 2% lipid, and 26 ± 2% polysaccharide.

3.2 | Hydrophobicity

Hydrophobicity of the bacterial cell surface can be assumed to originate from nonpolar hydrocarbon functionalities in different types of macromolecules that build up the cell envelope. We previously compared data from cryo-XPS C 1s spectra to results from the traditional MATH assay (representing a partitioning of cells between an aqueous phase and an organic phase; Figure 3) for a range of planktonic bacterial cells grown on culture plates (*E. coli* lipopolysaccharide mutants).[21] This comparison showed that the ratio between nonpolar C (with bonds to other C and/or H) and total carbon in C 1s spectra follow the same trend as data obtained from the MATH assay for all strains except one (RN106).[21]

Based on the results from the XPS analyses, the planktonic strains mentioned in this article increase in hydrophobicity in the order: River isolate *R. aquatilis* ≤ *P. fluorescens* (DSM50090) < *ΔpJN2133* < *P. fluorescens*

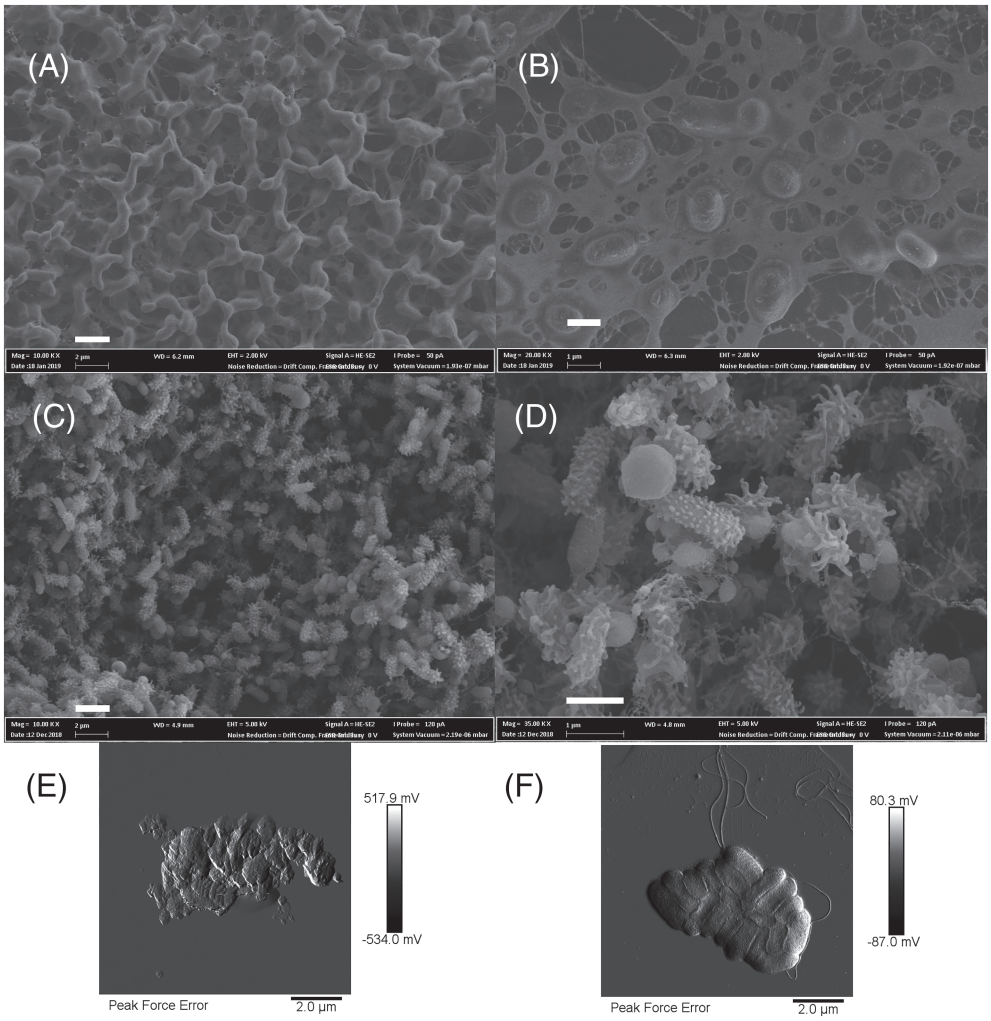

FIGURE 1 *R. aquatilis* imaged using cryo-SEM (A and B), regular SEM (C and D), and atomic force microscopy (AFM) (E and F). Scale bars represent 2 µm in A, C, D, and F, as well as 1 µm in B and D. AFM imaging of *R. aquatilis* (E) before and (F) after washing. AFM images show that extracellular polymeric substances observed in SEM is removed to a large extent by washing to uncover rod-shaped cells with flagella. (The clustering of cells in AFM images is most likely a consequence of centrifugation being part of the washing procedure.)

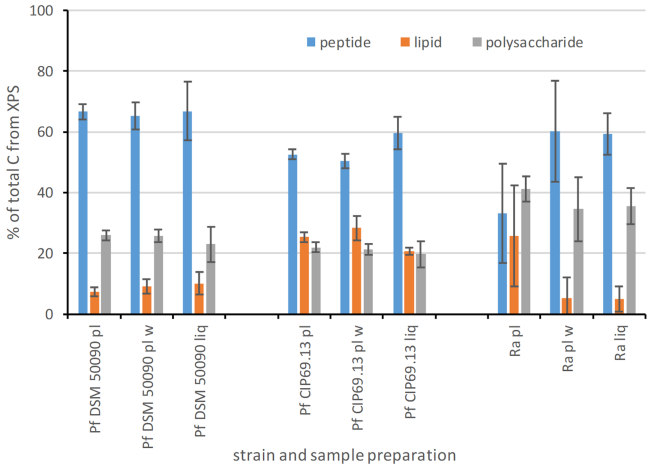

FIGURE 2 Surface composition as predicted from cryo-XPS C 1s spectra of bacteria grown on nutrient agar (pl) as well as in liquid broth (liq). Cells in liquid broth were always rinsed with phosphate buffered saline. Samples from plates were measured both washed (pl w) and nonwashed (pl). Pf = *P. fluorescens*, Ra = *R. aquatilis*. Each bar represent at least two biological replicates (n = 2–5). Data from model with spectral components

(CIP69.13) < *ΔpelA* = *ΔwspF* < PAO1 (Table 3). This comparison indicates that the first two strains were more hydrophilic than the previously described *E. coli* strains, whereas the PAO1 strains would be of similar hydrophobicity as the *E. coli* strains reported by Nakao et al.[21]

3.3 | Bacterial biofilms

To study how differences in EPS influence XPS data of biofilms, we selected four different strains from *P. aeruginosa*, ie, the lab strain PAO1 (wild type, here labeled PAO1) and three mutants of PAO1 that were expected to have differences in EPS secretion. The *ΔpelA* mutant is deficient in the synthesis of an EPS polysaccharide involved in biofilm formation for nonmucoid strains (ie, does also not produce alginate) of *P. aerugionsa*.[19,29] The remaining two mutants were chosen as they express low (*ΔpJN2133*) or high (*ΔwspF*) levels of a signaling molecule (c-di-GMP) known to influence many pathways in the bacterial cell including EPS secretion as well as biofilm formation.[20] In order to differentiate between the signal from the bacterial cell and EPS, we compared biofilm data to data from planktonic cells grown on culture plates. A significant difference ($p < 0.05$) in peptide and lipid

TABLE 2 Statistical comparisons between sample groups and *p*-values from the students *T* test

Sample	Peptide	Lipid	Polysaccharide
R. aquatilis [a]			
pl vs pl w	0.115	0.121	0.364
pl vs liq	0.062	0.106	0.250
pl w vs liq	0.945	0.960	0.892
P. fluorescens (DSM50090)[a]			
pl vs pl w	0.574	0.261	0.873
pl vs liq	0.966	0.233	0.346
liq vs pl w	0.745	0.639	0.356
P. fluorescens (CIP69.13)[a]			
pl vs pl w	0.233	0.247	0.661
pl vs liq	0.056	0.022	0.363
liq vs pl w	0.156	0.126	0.676
Strain comparison			
DSM50090 vs CIP69.13	0.000	0.000	0.003
DSM50090 vs *R. aquatilis*	0.015	0.440	0.000
CIP69.13 vs *R. aquatilis*	0.661	0.021	0.000
Biofilms after 12 h vs 15 h			
PAO1	0.408	0.180	0.133
ΔpelA	0.005	0.021	0.969
ΔpJN2133	0.898	0.552	0.157
ΔwspF	0.094	0.180	0.050
15 h biofilm vs planktonic			
PAO1	0.001	0.003	0.163
ΔpelA	0.001	0.003	0.075
ΔpJN2133	0.059	0.077	0.044
ΔwspF	0.001	0.001	0.286
12 h biofilm vs planktonic			
PAO1	0.005	0.031	0.005
ΔpelA	0.001	0.002	0.013
ΔpJN2133	0.136	0.070	0.660
ΔwspF	0.042	0.025	0.126

[a]Bacteria grown in liquid broth (liq), on culture plates (pl), bacteria on culture plate that were subsequently washed (pl w).

concentration was observed for three of the strains between the biofilms and the planktonic cells, ie, PAO1, *ΔpelA*, and *ΔwspF* (Figure 4 and Table 2). However, the difference was less significant for the *ΔpJN2133* strain. No significant difference between data points after 12 and 15 h of growth was observed except for *ΔpelA*. Neither did the thickness of the biofilms (as reflected in signal form the glass substrate, ie, Si 2p) appear to change significantly ($p > 0.2$ for all samples) between 12 and 15 h. The difference observed between planktonic cells and biofilms are interpreted as caused by increased EPS production in the biofilm compared with in growth on culture plates. The *ΔpJN2133* strain has been reported to have low c-di-GMP and be a weak biofilm former, which could explain the closer resemblance between biofilms and planktonic cells for this strain.[20] The peptide component appears to be dominating at the biofilm surface whereas the amount of lipid-like substances is higher for cells grown on culture plates. Future studies, for example, using confocal microscopy and staining may explain these observed compositional changes at the surface of biofilms.

3.4 | Bacterial outer-membrane vesicles

Small membrane structures such as OMVs can be analyzed with cryo-XPS and their composition compared with that of their parent strain. To this aim, we analyzed OMVs and parent bacteria from two *E. coli* strains.[21] In Figure 5, it can clearly be seen that the OMVs consist of relatively higher amounts of lipids ($p < 0.05$) for both strains. The *ΔflhD ΔwaaL* OMVs also showed reduced peptide content, which may represent a reduction in protein and/or peptidoglycan. This may either represent a reduction in outer membrane proteins caused by some

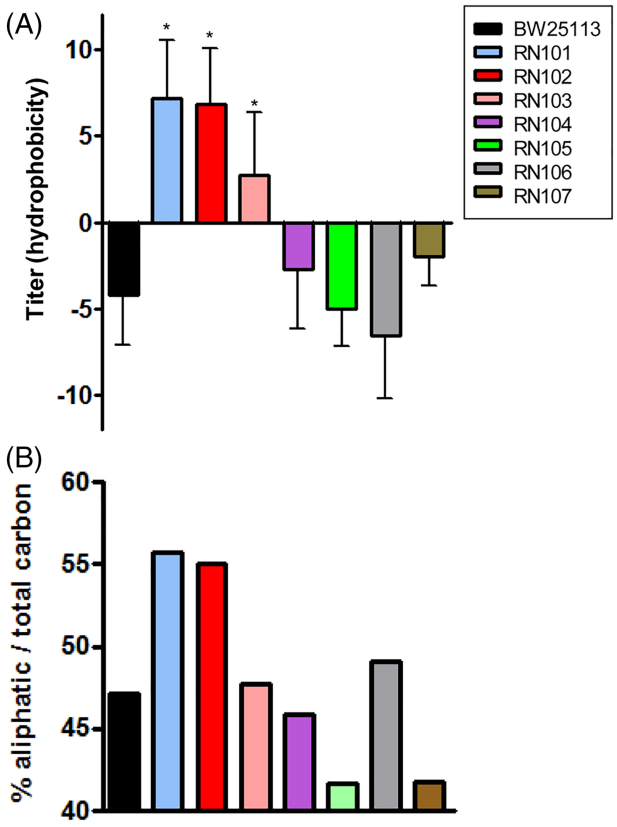

FIGURE 3 Comparison of surface hydrophobicity using (A) partitioning of cells between hexadecane and water (MATH assay) and (B) ratio of nonpolar carbon to total carbon, for eight strains of *Escherichia coli*. The black bar represents wild-type BW25113, and the colored bars represent different mutants in the lipopolysaccharide synthesis. Copyright 2012 Nakao et al[21] reprinted under Creative Commons Attribution License

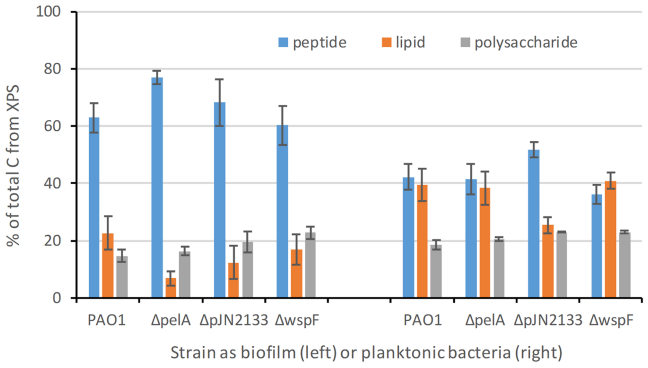

FIGURE 4 Average constituent concentration for the surface of biofilms grown for 12 and 15 h (average of six points distributed on two biological replicates (12 and 15 h), n = 6) as well as planktonic cells (from culture plates, two biological replicates, n = 2) for four *P. aeruginosa* strains. The prediction is based on fitting the C 1s peak using three spectral components representing peptide (protein and peptidoglycan), lipid, and polysaccharide[6]

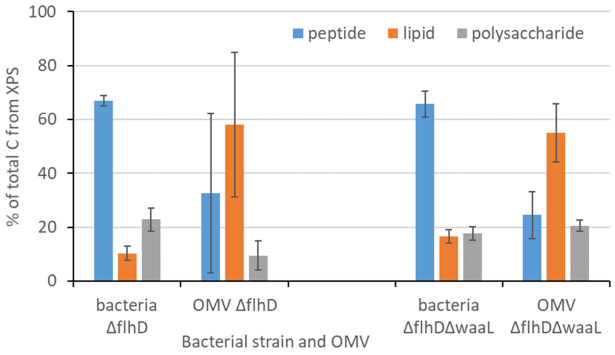

FIGURE 5 Average constituent concentration based on C 1s spectra from *E. coli* bacteria and outer-membrane vesicles (OMVs). Significant difference between parent strain ($p < 0.05$) and OMV was found only for the lipid and polysaccharide component in the *ΔflhD* mutant and for the peptide and lipid components for the *ΔflhD ΔwaaL* double mutant shown above (n = 3 for both *ΔflhD* samples, n = 2 for both *ΔflhD ΔwaaL* samples). Data from model with spectral components

sorting mechanisms during vesicle budding or that the budding leaves behind some of the peptidoglycan layer that is probed when the entire cell is analyzed.[6,10] It is worth noting, though, that peptidoglycan has been detected inside OMVs in some bacteria.[30] Previous work have shown that in order to separate the contribution of protein and peptidoglycan, XPS analyses can be combined with separate protein quantification using the Bradford assay.[30,31] These data suggest that cryo-XPS may be used as a tool to study compositional changes between the cell membrane and vesicles during vesicle genesis.

4 | COMPARISON BETWEEN DATA-TREATMENT METHODS

Decomposition of C 1s spectra from cryo-XPS analyses of fast-frozen bacterial systems can be performed using either Equation 2a to 2c,

TABLE 3 Percentage of nonpolar C of total C in C1s of XPS spectra of planktonic bacterial strains

Species	Strain	% Nonpolar C of Total C	Standard Deviation (Number of Replicates)
R. aquatilis	AH0123	33	4 (9)
P. fluorescens	DSM50090	37	2 (11)
P. fluorescens	CIP69.13	45	2 (8)
P. aeruginosa	PAO1 *ΔpJN2133*	43	1 (2)
P. aeruginosa	PAO1 *ΔpelA*	53	2 (2)
P. aeruginosa	PAO1 *ΔwspF*	53	0.4 (2)
P. aeruginosa	PAO1	55	2 (2)

described in the introduction, or the multivariate curve fitting approach that we developed and published in 2011.[5,6] To compare these two methods, we applied them side by side on the dataset presented in this article (Figure 6). The trends confirm what we previously reported for a dataset originating from samples of *Bacillus subtillis*.[5,16] The peptide composition obtained from the spectral components is generally higher than what is derived using Equation 2a to 2c (Figure 6B,D). The opposite is observed for the lipid content, and the polysaccharide content is the most closely correlated between the two methods. However, Figure 6 shows that the relationship is far from linear. The reason for this lack of correlation may relate to the underlying assumptions of each method. The equation system is based on a peak intensity ratio for model compounds. The mathematical components are derived from multivariate curve resolution of a collection of 42 samples (including standards) with differences in surface composition. Thus, both data-treatment methods assume an "ideal" composition for the cell-envelope building blocks (lipid, peptide, and polysaccharide). However, the scatter in Figure 6 indicates that these "ideal" substances are not identical between the two methods. Equations 2a to 2c assume that the peak at 285.0 eV consists of intensity from peptide and hydrocarbon at a ratio of 0.4:1, the peak at 286.5 eV of peptide and polysaccharide at a ratio of ~0.3:0.8, and the peak at 288.2 eV of peptide and polysaccharide at a ratio of ~0.3:0.2. On the other hand, the shape of the spectral components (Figure 6A) summarizes intensities from all three components throughout the width of the peak. The polysaccharide spectral component includes some adventitious hydrocarbon at 285.0 eV. Furthermore, the ideal hydrocarbon in the equation system and lipid spectral component differs in that the latter also includes a contribution form ester or carboxylic groups around 287 and 289 eV. These differences

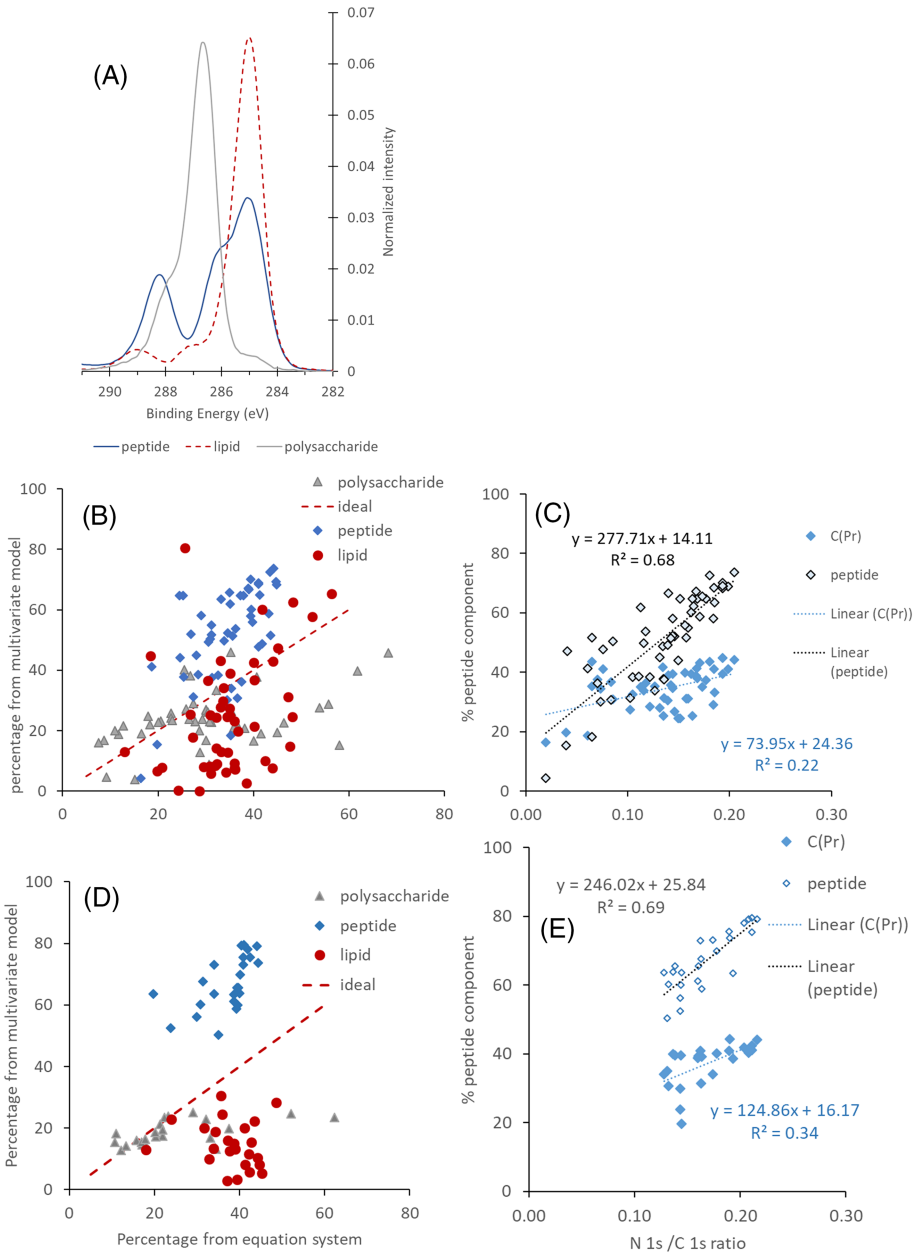

FIGURE 6 A, Shape of the three spectral components used in to fit C 1s spectra in the multivariate model. The solid blue line represents peptide component, the broken red line represents lipid, and the grey solid line represents polysaccharide.[6] B and D, Correlation between percentages derived from data treatment using equation system 2 and the fitting of spectral for (B) planktonic cells and vesicle samples, as well as (D) biofilm samples. The solid red line represents an ideal agreement between the two methods. C and E, Correlation of the N 1s/C 1s ratio vs percentage of peptide component derived from the two data treatment methods for (C) planktonic and vesicle samples, as well as (E) biofilms samples. The empty diamonds represent the multivariate model, and the blue solid diamonds represent the Equations 2a-2c

probably can account for some of the nonlinear correlation observed between these two data-treatment methods. The higher peptide content that is generally obtained using the spectral components may be due to carbon atoms with a neighboring N being more readily captured using the spectral components, than they would be from fitting the C 1s spectrum with single Gaussian-Lorentzian peaks at 285.0 and 286.5 eV and thereafter using Equations 2a to 2c. Due to the large overlap of the peptide and lipid components in both data-treatment method, it is not surprising that as the relative content of peptide increases, the lipid component decreases. The spectral peptide component has previously been shown to correlate well with the N content of the sample surface, and it was suggested that this could be used as an "independent" validation of the peptide composition at the surface.[6] Also, in this dataset, we observe that the content of N (represented by the N1s/C1s ratio) correlates to peptide content from both data-treatment methods. However, the peptide data seem to spread over a larger range giving rise to a more steep slope and the obtained R^2 was found to be higher for the method using spectral components (R^2 = 0.68 or 0.69 vs R^2 = 0.22 or 0.34 for planktonic and vesicle, or biofilm samples) than for Equations 2a to 2c (Figure 6C,E). The fact that these two data treatment methods assume slightly different "ideal" building blocks suggests that they are complementary but not directly comparable. In some bacterial systems, a number of substances may be present at the surface of the sample that are far from the ideal building blocks used in the two models, for example, extracellular DNA. These are not estimated in any of the models but may influence the obtained percentages from the two models differently. In this current dataset, we did not observe differences between the correlation data from biofilms and planktonic cells (Figure 6). However, this may well be the case for other systems. Thus, it may be advisable to use both data treatment methods in combination.

5 | CONCLUSIONS

Cryo-XPS can successfully be used to study the surface chemistry of a range of bacterial systems using a similar methodological approach. We have shown that the C 1s spectrum can give a measure of the hydrophobicity of the bacterial cell surface, as well as information about surface composition of lipids, polysaccharides, and peptides (protein and/or peptidoglycan). From the methodological perspective, we observed that bacterial cells grown in liquid medium and on culture plates give rise to similar chemical composition, unless strains produce large amounts of EPS. Differences in surface composition were observed between planktonic cells, OMVs, and biofilms, showing that cryo-XPS can be a valuable tool to investigate, eg, production of EPS from bacterial cells, the composition of biofilm matrix in different types of biofilm, and membrane processes connected to OMV formation. Furthermore, we compared two published data treatment methods applicable to cryo-XPS data. We conclude that they are not correlated but give roughly similar estimates of surface composition. In general, the obtained polysaccharide content corresponded fairly well between the data-treatment methods, but the peptide content was higher when using spectral components than when using Equations 2a to 2c. The opposite was found for the lipid content. Independent validation using the N 1s/C 1s ratio and the peptide component suggests a higher correlation with the spectral components compared with Equations 2a to 2c. However, the two methods are complementary and depending on research question one may be preferred over the other.

Cryo-XPS is a powerful method to study surface compositional changes of biological systems as it maintains water within the cell structure. This fast-frozen water plays an important role to preserve the structural organization of the bacterial sample enabling analyses at conditions more close to what is observed in ambient conditions.[5] Recently, near-ambient pressure–XPS has been applied to bacterial cells.[32] We hypothesize that this method and cryo-XPS should give comparable data. However, to investigate this, future work should be undertaken to show to what extent data from cryo-XPS and NAP-XPS overlap.

ACKNOWLEDGEMENTS

The authors would like to acknowledge the Kempe Foundation (JCK-1720) and Formas (2017-00403) for funding parts of this study. Fabienne Quilés at LCPME in Nancy, France, and Marit Kjaervik at BAM in Berlin, Germany, are acknowledged for generously providing *P. fluorescens* strains. PAO1 mutants were generously provided by Caroline Harwoods lab, University of Washington, USA. Bernt Eric Uhlin generously provided the *E. coli* strains. Ryoma Nakao, National Institute of Infectious Disease, Tokyo, Japan, Sun Nyunt Wai and Bernt Eric Uhlin, Umeå University, Sweden, are greatly acknowledged for the initial cryo-XPS collaborations including a large library of *E. coli* mutants as well as fruitful discussions throughout the years. We are grateful to the anonymous reviewers for insightful comments helping us to improve the manuscript. The National Microscopy Infrastructure, NMI (VR-RFI 2016-00968), and Nikki Lee is acknowledged for SEM analyses. XPS analyses were performed at the XPS platform at Umeå University, Sweden.

ORCID

Olena Rzhepishevska https://orcid.org/0000-0002-7912-7447
Anastasiia Semenets https://orcid.org/0000-0002-6223-9506
David A. Cisneros https://orcid.org/0000-0001-9919-0075
Madeleine Ramstedt https://orcid.org/0000-0003-2646-8501

REFERENCES

1. Berne C, Ellison CK, Ducret A, Brun YV. Bacterial adhesion at the single-cell level. *Nat Rev Microbiol*. 2018;16(10):616-627.
2. Karatan E, Watnick P. Signals, regulatory networks, and materials that build and break bacterial biofilms. In. *Microbiol Mol Biol Rev*. 2009;73. United States(2):310-347.
3. Moriarty T, Poulsson A, Rochford ETJ, Richards RG. Bacterial adhesion and biomaterial surfaces. In: Ducheyne P, ed. *Comprehensive Biomaterials*. 1st ed. Vol.4 Amsterdam, Netherlands: Elsevier Science; 2011:75-100.
4. Ploux L, Ponche A, Anselme K. Bacteria/material interfaces: role of the material and cell wall properties. *J Adhes Sci Technol*. 2010;24 (13–14):2165-2201.

5. Ramstedt M, Leone L, Persson P, Shchukarev A. Cell wall composition of Bacillus subtilis changes as a function of pH and Zn^{2+} exposure: insights from cryo-XPS measurements. *Langmuir*. 2014;30(15):4367-4374.
6. Ramstedt M, Nakao R, Wai S, Uhlin B, Boily J. Monitoring surface chemical changes in the bacterial cell wall—multivariate analysis of cryo-X-ray photoelectron spectroscopy data. *J Biol Chem*. 2011;286(14):12389-12396.
7. Flemming H-C, Wingender J, Szewzyk U, Steinberg P, Rice SA, Kjelleberg S. Biofilms: an emergent form of bacterial life. *Nat Rev Microbiol*. 2016;14(9):563-575.
8. Hall-Stoodley L, Costerton JW, Stoodley P. Bacterial biofilms: from the natural environment to infectious diseases. *Nat Rev Microbiol*. 2004;2(2):95-108.
9. Jeanson S, Floury J, Gagnaire V, Lortal S, Thierry A. Bacterial colonies in solid media and foods: a review on their growth and interactions with the micro-environment. *Front Microbiol*. 2015;6:1284-1284.
10. Schwechheimer C, Kuehn MJ. Outer-membrane vesicles from Gram-negative bacteria: biogenesis and functions. *Nat Rev Microbiol*. 2015;13(10):605-619.
11. Kim JH, Lee J, Park J, Gho YS. Gram-negative and Gram-positive bacterial extracellular vesicles. *Semin Cell Dev Biol*. 2015;40:97-104.
12. Liu Y, Defourny KAY, Smid EJ, Abee T. Gram-positive bacterial extracellular vesicles and their impact on health and disease. *Front Microbiol*. 2018;9:1502. https://doi.org/10.3389/fmicb.2018.01502
13. Millard MM, Scherrer R, Thomas RS. Surface analysis and depth profile composition of bacterial cells by x-ray photoelectron spectroscopy and oxygen plasma etching. *Biochem Biophys Res Commun*. 1976;72(3):1209-1217.
14. van der Mei H, de Vries J, Busscher H. X-ray photoelectron spectroscopy for the study of microbial cell surfaces. *Surf Sci Rep*. 2000;39(1):3-24.
15. Rouxhet P, Genet M. XPS analysis of bio-organic systems. *Surf Interface Anal*. 2011;43(12):1453-1470.
16. Ramstedt M, Leone L, Shchukarev A. Bacterial surfaces in geochemistry—How can X-ray photoelectron spectroscopy help? In: Alessi DS, Veeramani H, Kenney JPL, eds. *Analytical Geomicrobiology: A Handbook of Instrumental Techniques*. Cambridge: Cambridge University Press; 2019:262-287.
17. Shchukarev A, Ramstedt M. Cryo-XPS: probing intact interfaces in nature and life. *Surf Interface Anal*. 2017;49(4):349-356.
18. Güvener ZT, Harwood CS. Subcellular location characteristics of the *Pseudomonas aeruginosa* GGDEF protein, WspR, indicate that it produces cyclic-di-GMP in response to growth on surfaces. *Mol Microbiol*. 2007;66(6):1459-1473.
19. Starkey M, Hickman JH, Ma L, et al. *Pseudomonas aeruginosa* Rugose small-Colony variants have adaptations that likely promote persistence in the cystic fibrosis lung. *J Bacteriol*. 2009;191(11):3492-3503.
20. Hickman JW, Tifrea DF, Harwood CS. A chemosensory system that regulates biofilm formation through modulation of cyclic diguanylate levels. *Proc Natl Acad Sci U S A*. 2005;102(40):14422-14427.
21. Nakao R, Ramstedt M, Wai SN, Uhlin BE. Enhanced biofilm formation by *Escherichia coli* LPS mutants defective in Hep biosynthesis. *PLoS ONE*. 2012;7. United States(12):e51241. https://doi.irg/10.1371/journal.pone.0051241
22. Reasoner DJ, Geldreich EE. A new medium for the enumeration and subculture of bacteria from potable water. *Appl Environ Microbiol*. 1985;49(1):1-7.
23. Ramstedt M, Shchukarev A. Analysis of bacterial cell surface chemical composition using cryogenic X-ray photoelectron spectroscopy. In: Hong H-J, ed. *Bacterial Cell Wall Homeostasis: Methods and Protocols*. New York, NY: Springer New York; 2016:215-223.
24. Wai SN, Takade A, Amako K, The release of outermembrane vesicles from the strains of enterotoxigenic Escherichia coli. *Microbiol. Immunol*. 1995;3:451-456.
25. Mikkelsen H, Duck Z, Lilley KS, Welch M. Interrelationships between colonies, biofilms, and planktonic cells of *Pseudomonas aeruginosa*. *J Bacteriol*. 2007;189(6):2411-2416.
26. Pintado ME, Pintado AIE, Malcata FX. Production of polysaccharide by *Rahnella aquatilis* with whey feedstock. *J Food Sci*. 1999;64(2):348-352.
27. Vyas P, Joshi R, Sharma K, Rahi P, Gulati A, Gulati A. Cold-adapted and Rhizosphere-competent strain of Rahnella sp. with broad-spectrum plant growth-promotion potential. *J Microbiol Biotechnol*. 2010;20(12):1724-1734.
28. Kim KY, Jordan D, Krishnan HB. Expression of genes from *Rahnella aquatilis* that are necessary for mineral phosphate solubilization in Escherichia coli. *FEMS Microbiol Lett*. 1998;159(1):121-127.
29. Colvin KM, Irie Y, Tart CS, et al. The Pel and Psl polysaccharides provide *Pseudomonas aeruginosa* structural redundancy within the biofilm matrix. *Environ Microbiol*. 2012;14(8):1913-1928.
30. Bielig H, Rompikuntal P, Dongre M, et al. NOD-like receptor activation by outer membrane vesicles from *Vibrio cholerae* non-O1 non-O139 strains is modulated by the quorum-sensing regulator HapR. *Infect Immun*. 2011;79(4):1418-1427.
31. Bradford MM. A rapid and sensitive method for the quantitation of microgram quantities of protein utilizing the principle of protein-dye binding. *Anal Biochem*. 1976;72(1):248-254.
32. Kjærvik M, Schwibbert K, Dietrich P, Thissen A, Unger WES. Surface characterisation of Escherichia coli under various conditions by near-ambient pressure XPS. *Surf Interface Anal*. 2018;50(11):996-1000.

How to cite this article: Hagberg A, Rzhepishevska O, Semenets A, Cisneros DA, Ramstedt M. Surface analysis of bacterial systems using cryo-X-ray photoelectron spectroscopy. *Surf Interface Anal*. 2020;52:792–801. https://doi.org/10.1002/sia.6854